Journal of Solid State Electrochemistry
https://doi.org/10.1007/s10008-018-3979-y

ORIGINAL PAPER

A highly sensitive sensor of paracetamol based on zinc-layered hydroxide-*L*-phenylalanate-modified multiwalled carbon nanotube paste electrode

Mohamad Syahrizal Ahmad[1,2] · Illyas Md Isa[1,2] · Norhayati Hashim[1,2] · Suyanta M. Si[3] · Mohamad Idris Saidin[4]

Received: 22 March 2018 / Revised: 25 April 2018 / Accepted: 26 April 2018

Abstract
A new zinc-layered hydroxide-*L*-phenylalanate (ZLH-LP)-modified multiwalled carbon nanotube (MWCNT) was prepared as a new material of paste electrode for the detection of paracetamol (PCM) in 1.0×10^{-1} M phosphate buffer solution and at pH 7.5. The electrochemical characterization of the MWCNTs/ZLH-LP paste electrode was characterized by square wave voltammetry, electrochemical impedance spectroscopy, and cyclic voltammetry while the morphology properties of the MWCNTs, ZLH-LP, and MWCNTs/ZLH-LP were investigated using transmission electron microscopy and scanning electron microscopy. Under optimized conditions, the MWCNTs/ZLH-LP paste electrode demonstrated an excellent electrocatalytic activity towards oxidation of PCM in the linear responses' ranges from 7.0×10^{-7} M to 1.0×10^{-4} M (correlation coefficient, 0.996) with the limit of detection obtained at 8.3×10^{-8} M. As a conclusion, the MWCNTs/ZLH-LP paste electrode revealed good repeatability, reproducibility, and stability, and was found to be applicable for use in pharmaceutical tablet samples.

Keywords Paracetamol · Multiwalled carbon nanotubes · Square wave voltammetry · Chronocoulometry · Zinc layered hydroxide-*L*-phenylalanate

Introduction

Paracetamol (PCM, Fig. 1) was first introduced into medicine in 1893 by Von Mering. It is one of the most widely used antipyretics by sedating the center of hypothalamic heat-regulating and an analgesic by inhibiting the preparation of prostaglandin in the central nervous system [1, 2]. It can be used as an alternative for the people who are sensitive to aspirin or acetylsalicylic acid [3]. At therapeutic level, PCM is generally considered effective and safe for normal drug users [4]. However, non-prescribed high-dose consumption of PCM leads to the toxic metabolites' accumulation, which causes severe and sometimes fatal nephrotoxicity and hepatoxicity [5, 6]. In the United States of America (USA), most acute liver failure cases annually are caused by PCM or idiosyncratic drug reactions [7]. Thus, development of an analytical method for simple and accurate analysis of PCM is important.

One of the significant parts in analytical chemistry is analysis of the drug, which plays an important role in quality control of the drug in pharmaceutical, medicinal, and clinical chemistry. Variety methods have been established for determining PCM in biological fluids and pharmaceutical tablets such as titrimetry [8], capillary electrophoresis [9], colorimetry [10], chromatography [11, 12], flow-injection analysis [13], Fourier transform infrared spectroscopy [14], spectrophotometry [15, 16], and chemiluminescence [17]. Unfortunately, these listed methods are high costs, consume a long time for the analysis, and sometimes need complicated sample pre-treatments and to be handled by experienced

✉ Illyas Md Isa
illyas@fsmt.upsi.edu.my

[1] Nanotechnology Research Centre, Faculty of Science and Mathematics, Sultan Idris Education University, 35900 Tanjung Malim, Perak, Malaysia

[2] Department of Chemistry, Faculty of Science and Mathematics, Sultan Idris Education University, 35900 Tanjung Malim, Perak, Malaysia

[3] Department of Chemistry Education, Faculty of Mathematics and Natural Science, Yogyakarta State University, Yogyakarta, Indonesia

[4] Advanced Analytical Services Laboratory, MIMOS Bhd., Technology Park of Malaysia, 57000 Kuala Lumpur, Malaysia

Published online: 09 May 2018

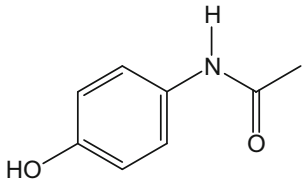

Fig. 1 Structure of PCM

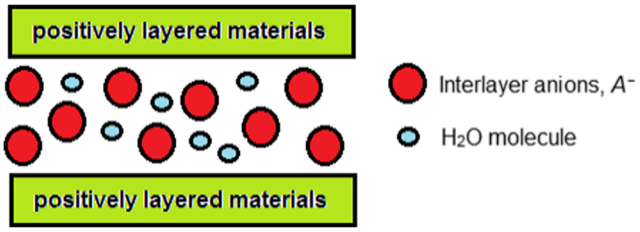

Scheme 1 Illustration of layered hydroxide salts

operators that make it not suitable for routine analysis. Since PCM is one species that can be oxidized electrochemically to produce *N*-acetyl-*p*-quinoneimine (NAPQI) involving two electrons, electrochemical techniques can be considered as an interesting alternative to the above methods due to their advantageous and unique properties such as good sensitivity, simplicity, excellent catalytic activity, and easy fabrication [18, 19]. There are many researches with several combinations of electrode surfaces, modifiers, techniques, and methods that have been done to improve the selectivity and sensitivity for electroanalytical studies of PCM. For instances, Vidyadharan and co-workers used sensor based on Ni-doped Co ferrite modified with the carbon electrode for the sensitive detection of PCM [20]. In 2010, Pournaghi-Azar and his group members have studied the simultaneous voltammetry of PCM, codeine, and ascorbic acid using Al electrode surface modified with the thin layer of Pd [21]. Besides that, Tyszczuk-Rotko and his group introduced a novel sensor of a boron-doped diamond electrode modified with lead film and Nafion for determination of ascorbic acid and PCM simultaneously [22]. In 2012, Yang and co-workers tested different organic molecules as a modifier on glassy carbon electrodes for determination of PCM in acidic solution [23] while Raoof and his group members reported the using of ordered mesoporous carbon and hexagonal arrays of tubes for simultaneous determination of epinephrine and PCM [24].

Recently, various materials incorporated to carbon nanotubes (CNT) have received considerable interest in an electroanalysis field since their first discovery in 1991 [25]. CNT has specific and unique properties such as a higher electrical conductivity, its mechanical strength, larger surface area, and chemical stability [26–28]. Moreover, the subtle electronic behavior of CNT revealed that it has the tendency to promote the electron transfer reaction and has a high electrocatalytic effect when used as electrode materials [29, 30]. Metal-layered hydroxides with an empirical formula of $M^{2+}(OH)_{2-x}(A^{m-})_{x/m}{\cdot}mH_2O$, where M^{2+} is referring to the divalent metallic cations such as Zn^{2+}, Ni^{2+}, Mg^{2+}, and Mn^{2+} that form layered materials consisting of positively charged, while A^{m-} is ions with the negative charge that inserted between these layers as shown in Scheme 1, have been studied extensively and are recognized for their anion exchangeable properties [31]. The interlayer anions can be exchanged with organic or inorganic's charged compounds. Yin and his co-workers established a voltammetric sensor based on the combination of Au nanoparticles and an organophilic layered double hydroxide as a novel sensor for determination of PCM, dopamine, and 4-aminophenol [32]. Isa and his group members successfully fabricated Zn-layered hydroxide-3-(4-methoxyphenyl) propionate modified with the glassy carbon electrode as voltammetric sensor to detect the hydrazine in water samples [33]. Su et al. reported better electrochemical performance when MWCNT were mixed with the layered double hydroxide [34].

To the best of our knowledge, there is no research and study has been published reporting electrochemical detection of PCM using the MWCNT modified with ZLH-LP as a modifier as a voltammetric sensor. Thus, this study is intended to apply the MWCNT/ZLH-LP paste electrode as an alternative sensor for sensitive detection of PCM. Effective SWV parameters of the MWCNT/ZLH-LP paste electrode towards PCM determination were investigated in details and the results showed a good sensitivity, acceptable reproducibility and repeatability, low detection limit, wide linear dynamic range, and was successfully tested for the determination of PCM in pharmaceutical tablets with satisfactory results.

Experimental

Reagents and chemicals

All reagents and chemicals in this experiment were analytical grade and used without further purification. MWCNTs were ordered from Timesnano, China. PCM and KCl were obtained from Sigma-Aldrich, the USA. Generic tablets of paracetamol (0.5 g) were purchased from local pharmacy in Slim River, Perak. Different pH of phosphate buffer solutions (PBS) were prepared by mixing the stock solutions of 1.0×10^{-1} M KH_2PO_4 and 1.0×10^{-1} M K_2HPO_4 (Merck, Germany). Stock solutions of PCM (1.0×10^{-3} M) were freshly prepared by dissolving the PCM in deionized water and stored at 4 °C in the dark place until it to be used. The ZLH-LP was prepared in the laboratory as reported previously [31].

Instrumentation

Electrochemical impedance spectroscopy (EIS) and square wave voltammetry (SWV)/cyclic voltammetry (CV) were

performed with a Potentiostat/Galvanostat Ref 3000 model (USA) and Potentiostat Series-G750 (USA), respectively. The measurements were carried out using the conventional three-electrode cell consisting of a platinum wire as a counter or auxiliary electrode, an Ag/AgCl electrode MF-2052 model from Bioanalytical System, USA, as a reference electrode, and the MWCNT/ZLH-LP paste electrode as a working electrode. The surface morphological characterization of MWCNTs and MWCNTs/ZLH-LP were performed on the FESEM SU8020 UHR model from Hitachi, Japan.

The fabrication of the MWCNTs/ZLH-LP

For the fabrication of the MWCNTs/ZLH-LP paste electrode, 0.09 g MWCNTs and 0.01 g ZLH-LP were mixed with a suitable amount of paraffin oil in a mortar and pestle until the homogenized paste was produced. Then, the uniform paste was packed into the Teflon tube (3 cm long and 2-mm diameter) and a copper wire was inserted into one of the end of the carbon paste to establish the electrical contact. The surface of the paste was polished with weighing paper just before used. For electrochemical activity comparison, the unmodified MWCNT paste electrode was fabricated through a similar approach without the addition of ZLH-LP modifier.

Measurement procedure

The determination of PCM was performed by using SWV in 1.0×10^{-1} M PBS as supporting electrolyte and conditions were as follows: potential range = 0.0 V to + 0.6 V, step increment = 3 mV, pulse height = 60 mV, and frequency = 120 Hz. EIS study was carried out in 1.0×10^{-4} M PCM in the presence of 1.0×10^{-1} M PBS as supporting electrolyte. All the electrochemical experiments were conducted at 25± 1 °C and were measured against Ag/AgCl (reference electrode). For the detection of the PCM tablet in real sample analysis, the tablet was weighed and then ground, becoming a powder, followed by dissolving and diluting into 50 mL volumetric flask.

Result and discussion

Characterization of the MWCNTs and MWCNTs/ZLH-LP

The transmission electron microscopy (TEM) and scanning electron microscopy (SEM) were used to characterize the morphology of the fabricated paste electrode surface. Figure 2a displays the typical SEM image of MWCNTs as a porous network structure which is dense and highly entangled. After modification with the ZLH-LP, Fig. 2b indicates that the ZLH-LP was distributed on the MWCNTs with special three-dimensional (3D) structure. It was proven by the TEM image that shows ZLH-LP as a dark spot was covered by transparent tubes of MWCNTs (Fig. 2c). These results clearly revealed the successfully modified MWCNTs along with ZLH-LP, which increased the effective surface area of electrode and formed the conducive condition for PCM determination.

Electrochemical behaviors at the surface of the MWCNT/ZLH-LP and unmodified MWCNT paste electrodes were initially determined by CV in 1.0×10^{-3} M PCM in the presence of 1.0×10^{-1} M PBS at a scan rate ( ) of 100 mV s^{-1} as shown in Fig. 3. The unmodified MWCNT paste electrode showed a couple of redox peaks with differences between cathodic peak and anodic peak potentials or also known as the peak-to-peak separation (ΔE_p) of 0.33 V. The addition of the ZLH-LP increased significantly the peak current intensities and also decreased the ΔE_p to 0.14 V, suggesting that the addition of the ZLH-LP has improved the charge transfer rate. For reversible redox process, ΔE_p should be 0. The relatively small ΔE_p might arise from the effects of uncompensated ohmic drops and charge transfer [35].

The effects of the scan rates ( ) on the electrochemical behaviors of 1.0×10^{-3} M PCM in the presence of 1.0×10^{-1} M PBS at the MWCNT/ZLH-LP paste electrode were investigated to study the kinetic of reactions. Figure 4a shows the peak currents' oxidation of PCM increased with increasing from 10 to 200 mV s^{-1}. It can be seen clearly in Fig. 4b that plots of the peak current (I_p) vs. scan rate ( ) showed the straight lines with linear equations as, $I_{pa}/\mu A = + 0.11$ /mV s^{-1} + 1.92/μA

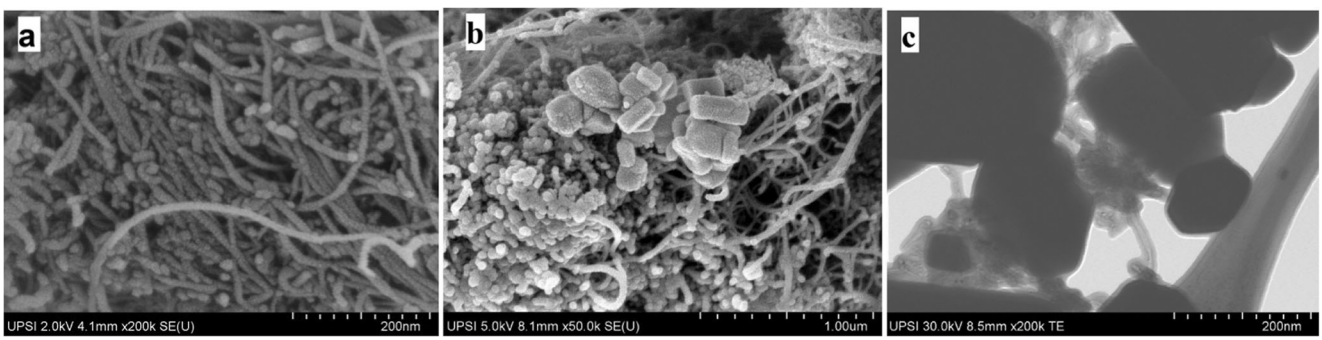

Fig. 2 The SEM image of **a** MWCNTs, **b** MWCNTs/ZLH-LP, and the TEM image of **c** MWCNTs/ZLH-LP

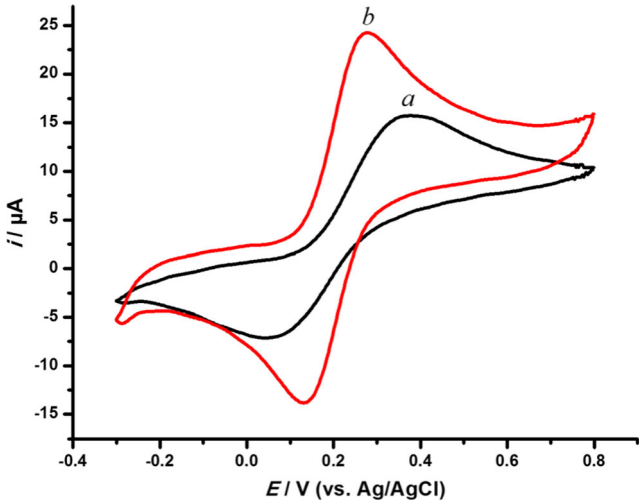

Fig. 3 Cyclic voltammogram of the (*a*) unmodified MWCNT and (*b*) MWCNT/ZLH-LP paste electrodes in 1.0×10^{-3} M PCM in the presence of 1.0×10^{-1} M PBS at the = 100 mV s^{-1}

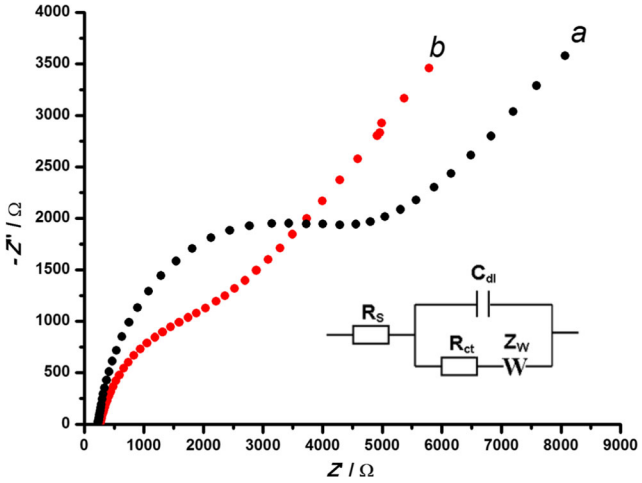

Fig. 5 EIS of the (*a*) unmodified MWCNT and (*b*) MWCNT/ZLH-LP paste electrodes in 1.0×10^{-4} M PCM in the presence of 1.0×10^{-1} M PBS. Inset: Randle's equivalent electrical circuit system

($R^2 = 0.994$) and $I_{pc}/\mu A = -0.07$ /mV s^{-1}–0.26/μA ($R^2 = 0.992$). These results suggested that the kinetic of the electrode reaction was predominantly adsorption-controlled process. Figure 4c shows the linear line for the plot of log I_{pa} as a function of log with the equation as log $I_{pa}/\mu A = +0.82$ log /mV s^{-1} + 0.53/μA ($R^2 = 0.992$). The obtained slope of 0.82 (theoretical value 1.0) confirmed that the kinetic of the electrode reaction was adsorption-controlled process [36]. The ΔE_p increased with increasing scan rate could be caused by uncompensated ohmic drops [37].

EIS is an effective tool to investigate the characteristics of the modified electrodes' interface. It provides some information including electron transfer resistance, impedance of electrode, and double layer capacitance. In Nyquist diagram, the

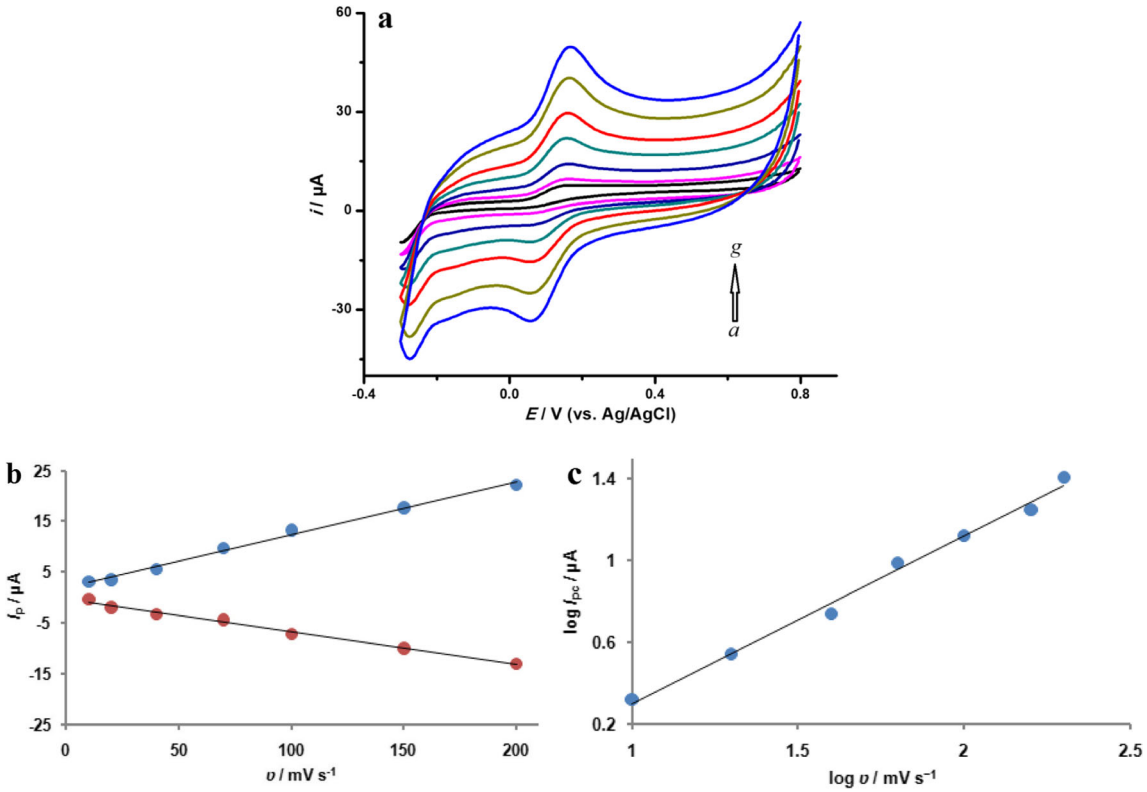

Fig. 4 **a** Cyclic voltammogram of the MWCNT/ZLH-LP paste electrode in 1.0×10^{-3} M PCM in the presence of 1.0×10^{-1} M PBS at a scan rate of (*a*) 10 mV s^{-1}, (*b*) 20 mV s^{-1}, (*c*) 40 mV s^{-1}, (*d*) 70 mV s^{-1}, (*e*) 100 mV s^{-1}, (*f*) 150 mV s^{-1}, and (*g*) 200 mV s^{-1}. **b** The plot of I_p vs. . **c** The plot of log I_{pa} vs. log

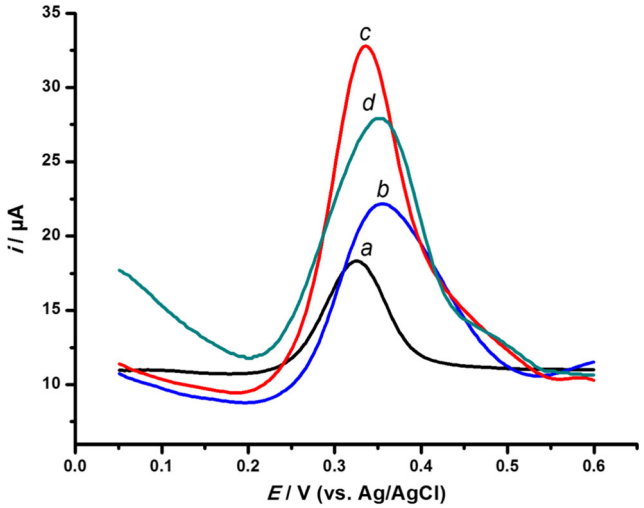

Fig. 6 The effect of (*a*) 0%, (*b*) 5%, (*c*) 10%, and (*d*) 15% composition of ZLH-LP on the peak current of 1.0×10^{-4} M PCM at $a = 60$ mV, $\Delta E_S = 5$ mV, and $f = 120$ Hz

diameter of the semicircle corresponded to the resistance of electron transfer (R_{ct}) which controls the kinetics of electron transfer at the interface of electrode, where a bigger radius of the semicircle is associated to a higher resistance value, while the linear part is equal to the diffusion process. Figure 5 shows the Nyquist plot for the MWCNT/ZLH-LP and unmodified MWCNT paste electrodes when these electrodes immersed in 1.0×10^{-4} M PCM containing 1.0×10^{-1} M PBS as a supporting electrode with frequencies ranging from 10^6 to 1 Hz. The results showed that the R_{ct} (3050 Ω) of the unmodified MWCNTs is larger than the R_{ct} (1250 Ω) of ZLH-LP/MWCNT paste electrodes which suggested that ZLH-LP/MWCNT paste electrode has faster electron-conducting ability and higher conductivity at the surface. From the R_{ct} data obtained, the electron transfer apparent rate constant, k_{app} for each electrode can be calculated in accordance with Eq. 1 to measure the kinetic facility of the redox pairs:

$$k_{app} = R\,T / F^2\,R_{ct}\,A\,C \quad (1)$$

where R = gas constant (J K^{-1} mol^{-1}), T = temperature (K), F = Faraday's constant (C mol^{-1}), R_{ct} = electron transfer resistance (Ω), A = electrode surface area (cm^2), and C = concentration of analyte (mol cm^{-3}). The k_{app} values obtained for the MWCNT/ZLH-LP and unmodified MWCNT paste electrodes were 3.4×10^{-5} cm s^{-1} and 6.2×10^{-5} cm s^{-1}, respectively. Thus, the greater value of k_{app} for the MWCNT/ZLH-LP paste electrode indicates a faster transfer of the electron for this paste electrode compared to the unmodified MWCNTs.

The effect of the composition of the ZLH-LP

The experiments were carried out to study the influence of the composition of the ZLH-LP on the oxidation peak current of PCM at pulse size (*a*) 60 mV, step size (ΔE_S) 5 mV, and frequency (*f*) 120 Hz. Zero, 5, 10, and 15% of ZLH-LP were modified with MWCNT, respectively. As can be seen in Fig. 6, when the amount of ZLH-LP increased from 0 to 10%, peak current intensities also increased until reached maximum capacity at 15%; it started to decrease the intensities of peak current. It was probably because the surface of electron transfer on the electrode was hindered which reduced the conductivity of the MWCNT/ZLH-LP paste electrode. Therefore, 10% composition of ZLH-LP modifier was chosen as the main electrode to carry out further research.

Chronocoulometry study

Chronocoulometry studies were carried out using 4.0×10^{-3} M $[Fe(CN)_6]^{3-/4-}$ consisting 1.0×10^{-1} M KCl as a

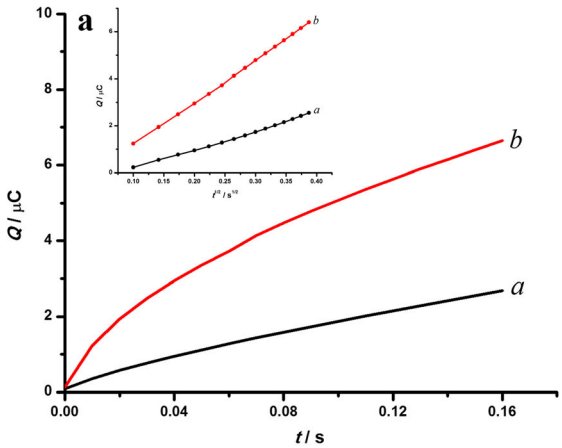

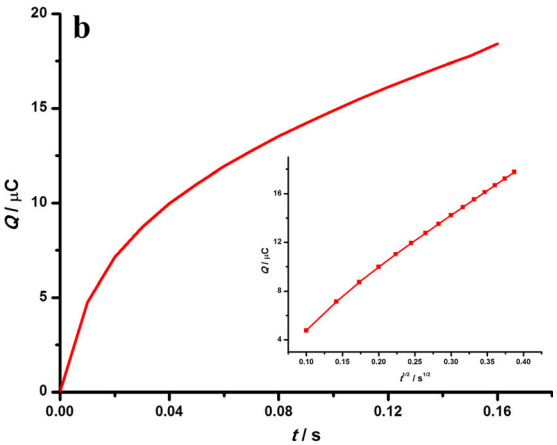

Fig. 7 **a** Plot of Q vs. t (inset: plot of Q vs. $t^{1/2}$) of the (*a*) unmodified MWCNT and (*b*) MWCNT/ZLH-LP paste electrodes in 4.0×10^{-3} M $[Fe(CN)_6]^{3-/4-}$ consisting 1.0×10^{-1} M KCl. **b** Plot of Q vs. t (inset: plot of Q vs. $t^{1/2}$) of the MWCNT/ZLH-LP paste electrode in 1.0×10^{-4} M PCM in 1.0×10^{-1} M PBS (pH 7.5) after background subtraction

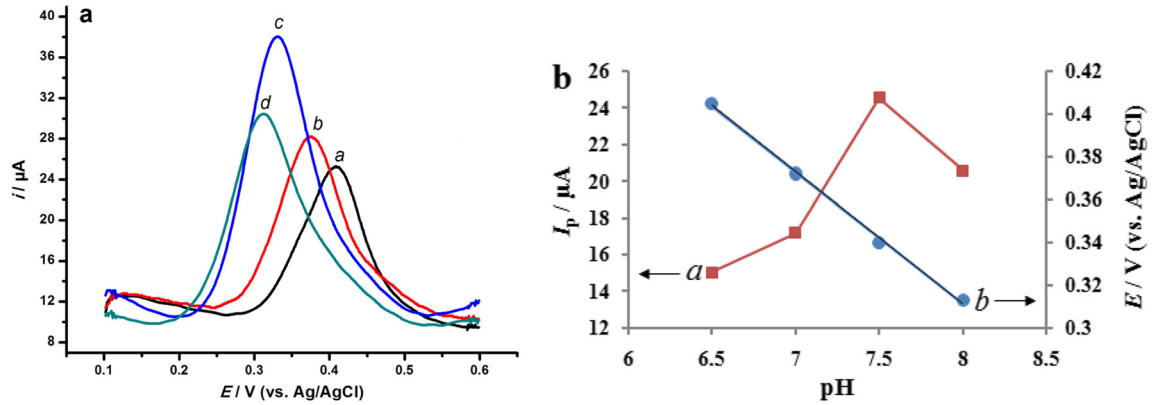

Fig. 8 **a** Effects of the pH on peak currents ($a = 40$ mV, $\Delta E_S = 6$ mV, $f = 120$ Hz). **b** The plot of I_p and E vs. pH

model complex to calculate the effective surface area (A) of the MWCNT/ZLH-LP and unmodified MWCNT paste electrodes according to Eq. 2 given by Anson [38]:

$$Q(t) = 2\,n\,A\,C\,F\,D^{1/2}\,t^{1/2}/\pi^{1/2} + Q_{dl} + Q_{ads} \quad (2)$$

where A = effective surface area of electrode (cm^2), Q_{ads} = Faradic charge, Q_{dl} = the double layer charge which is eliminated by background subtraction, D = standard diffusion coefficient of $[Fe(CN)_6]^{3-/4-}$ (7.6×10^{-6} cm^2 s^{-1}) [39] while n, t, C, and F have their usual meanings. From the slope of Q vs. $t^{1/2}$ (Fig. 7a), the calculated A of the MWCNT/ZLH-LP and unmodified MWCNT paste electrodes were 0.151 and 0.065 cm^2, respectively, which indicated the A increased (about twofold of unmodified MWCNTs) after the addition of ZLH-LP, leading to enhance the current responses towards $[Fe(CN)_6]^{3-/4-}$ for the

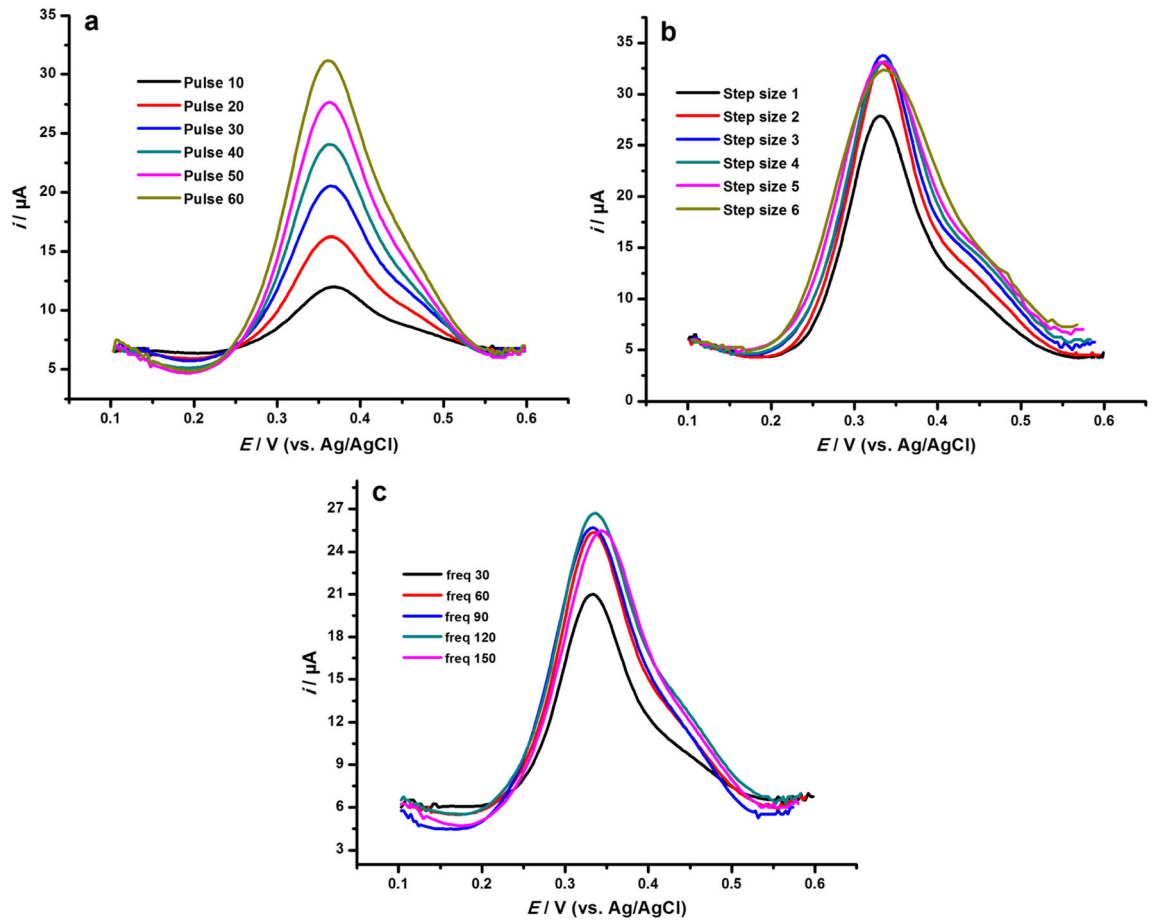

Fig. 9 Effect of the **a** pulse size ($\Delta E_S = 3$ mV, $f = 90$ Hz), **b** step size ($a = 3$ mV, $f = 90$ Hz), and **c** frequency ($\Delta E_S = 3$ mV, $a = 60$ mV) towards the peak currents of 1.0×10^{-4} M PCM in 1.0×10^{-1} M PBS

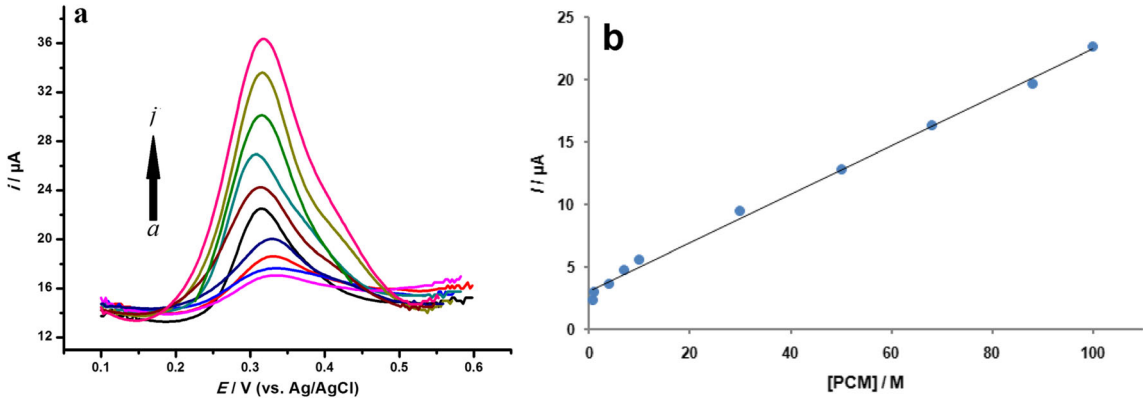

Fig. 10 **a** Square wave voltammogram of PCM using the MWCNT/ZLH-LP paste electrode on several PCM concentrations/M: (*a*) 7.0×10^{-7}, (*b*) 1.0×10^{-6}, (*c*) 4.0×10^{-6}, (*d*) 7.0×10^{-6}, (*e*) 1.0×10^{-5} (*f*) 3.0×10^{-5}, (*g*) 5.0×10^{-5}, (*h*) 7.0×10^{-5}, (*i*) 9.0×10^{-5}, and (*j*) 1.0×10^{-4}. **b** The calibration plot of PCM $a = 60$ mV, $\Delta E_S = 3$ mV, and $f = 120$ Hz

MWCNT/ZLH-LP paste electrode. Besides that, the Q_{ads} of PCM at the MWCNT/ZLH-LP paste electrode was also determined by chronocoulometry using 1.0×10^{-4} PCM in the presence of 1.0×10^{-1} M PBS and at pH 7.5. The Q_{ads} value can be estimated from the intercept of the plot of Q vs. $t^{1/2}$ as shown in Fig. 7b and found to be 9.3×10^{-7} C. Moreover, the adsorption capacity Γ was obtained to be 3.2×10^{-11} mol cm^{-2} according to Eq. 3 indicating the MWCNT/ZLH-LP paste electrode displayed a good adsorption capacity for PCM [40].

$$Q_{ads} = \Gamma n A F \quad (3)$$

Optimization of the experimental variables

The effects of pH

The electrochemical behaviors of PCM are usually depending on the pH value. Therefore, the effects of pH on the peak currents of the MWCNT/ZLH-LP paste electrode towards 1.0×10^{-4} M PCM in 1.0×10^{-1} M PBS were performed over the range of pH 6.5 to 8.0 at pulse size (*a*) 40 mV, step size (ΔE_S) 6 mV, and frequency (*f*) 120 Hz. Figure 8a, b (*a*) shows that the oxidation peak currents of PCM increased with increasing value of pH and reached its pH maximum at 7.5, and then, peak current starts to decrease from pH 8.0 suggesting that the oxidation reaction of PCM was kinetically more favorable at a lower pH [41]. Hence, pH 7.5 has been chosen as the optimum condition of experiments in order to get high sensitivity. In Fig. 8b (*b*), it can be seen that the peak potential (*E*) of PCM decreased with increasing the value of pH. The relationship between the value of peak potential (*E*) as a function of pH value at the MWCNT/ZLH-LP paste electrode can be expressed as $E/\text{V} = -0.061\ \text{pH} + 0.81/\text{V}$ ($R^2 = 0.998$). The slope obtained from the equation, 0.061, was close to the Nernst value (0.059 mV pH^{-1}) suggesting that the protons and electrons involved in the electrochemical process are equal [42].

The effects of SVW parameters

Based on Osteryoung, characteristic of SW voltammograms is depending on several parameters used. Therefore, the

Table 1 The efficiency comparison of the fabricated electrode in the electrocatalysis of PCM

Modifier/electrode	Method	Linear range (10^{-6} M)	LOD (10^{-6} M)	Ref.
Chitosan-copper-complex/multiwalled carbon nanotubes/GCE	DPV	1.0×10^{-7}–2.0×10^{-4}	2.4×10^{-8}	[43]
Au nanoparticles/poly(caffeic acid)/GCE	CV	2.0×10^{-7}–2.0×10^{-5}; 5.0×10^{-5}–1.0×10^{-3}	1.4×10^{-8}	[44]
Nickel-copper oxide/grapheme/GCE	SWV	4.0×10^{-6}–4.0×10^{-4}	1.3×10^{-6}	[45]
Nickel oxide nanoparticles-graphene oxide: epichlorohydrin/GCE	SWV	1.0×10^{-7}–2.9×10^{-6}	6.7×10^{-9}	[46]
Poly(caffeic acid)/GCE	SWV	2.0×10^{-7}–1.0×10^{-5}	2.6×10^{-8}	[47]
Bismuth oxide/SFE	DPV	5.0×10^{-7}–9.7×10^{-5}	3.0×10^{-8}	[48]
1-(4-bromobenzyl)-4-ferrocenyl-1H-(1,2,3)-triazole/GPE	SWV	1.0×10^{-5}–1.0×10^{-3}	8.1×10^{-6}	[49]
Cetylpyridinium bromide/MWCNT/CPE	DPV	5.0×10^{-6}–9.26×10^{-5}	5.7×10^{-7}	[50]
Poly(thionine)/MWCNT/CFE	DPV	2.5×10^{-5}–2.5×10^{-4}	6.0×10^{-6}	[51]
Zinc-layered hydroxide-*L*-phenylalanate/MWCNTs/CPE	SWV	7.0×10^{-7}–1.0×10^{-4}	8.3×10^{-8}	This work

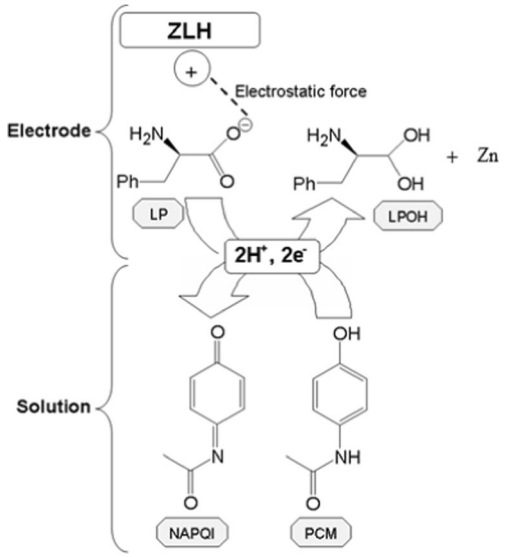

Scheme 2 Illustration of the proposed reaction mechanism at the MWCNT/ZLH-LP paste electrode and PCM solution

influence of SWV parameters such as pulse size (a), frequency (f), and step size (ΔE_S) towards the peak current of 1.0×10^{-4} M PCM in 1.0×10^{-1} M PBS (pH 7.5) was investigated to get the best sensitivity of the electrode. From Fig. 9a, it can be seen that the peak current intensities linearly increased with a slight shift to the more negative potential value as pulse size parameter increased from 10 to 60 mV with a step size and frequency fixed at 3 mV and 90 Hz, respectively. Pulse size above 60 mV started to give substantial broadening of the peak. Hence, pulse size 60 mV has been selected for further studies. Besides that, the effect of step size parameter was studied between 1 and 6 mV with a fixed pulse size and frequency at 60 mV and 60 Hz, respectively, as shown in Fig. 9b. Step size 3 mV was selected as it sets the highest sensitivity for PCM detection. Lastly, the peak currents were also found to vary with respect to the frequency (30 to 150 Hz) with a pulse size and step size fixed at 60 and 3 mV, respectively (Fig. 9c). The resultant peak currents increased as the frequency increased from 30 to 120 Hz before it started to decrease when the frequency is above 120 Hz. Thus, the 120 Hz of the frequency was taken for further investigations. As a conclusion, the values of pulse size, step size, and frequency were 60 mV, 3 mV, and 120 Hz, respectively, had been used as optimum parameter for calibration curve development.

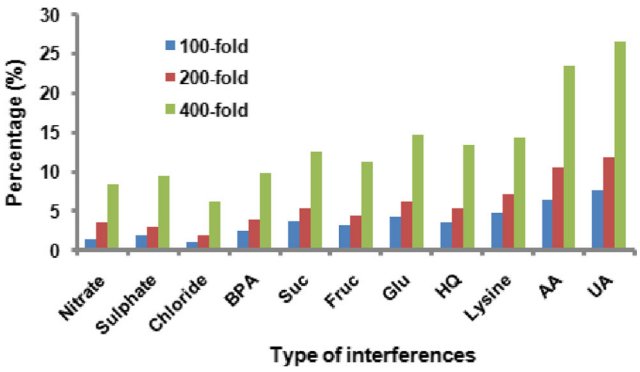

Fig. 11 The effect of interference substances to 1.0×10^{-4} M PCM

Calibration curve and limit of detection

Under the optimized condition of $a = 60$ mV, $\Delta E_S = 3$ mV, and $f = 120$ Hz, the SWV experiments were performed using the MWCNT/ZLH-LP paste electrode in various concentrations of PCM containing 1.0×10^{-1} M PBS (pH 7.5). Figure 10a displays the peak current increased with increasing the concentration of PCM. In addition, Fig. 10b shows clearly that the electrocatalytic peak current of PCM oxidation was linearly proportional to the concentrations of PCM in the range of 7.0×10^{-7} M to 1.0×10^{-4} M with the linear regression equation $I/\mu A = (0.19 \pm 0.01)$ [PCM]/μmol $L^{-1} + (3.07 \pm 0.13)/\mu A$ and the correlation coefficient (R^2) of 0.996. The limit of detection (LOD) for this experiment was calculated to be 8.3×10^{-8} M. These data obtained were compared with data reported by other published papers for electrocatalytic oxidation of PCM at the other mediators of the modified electrode as listed in Table 1. Scheme 2 illustrates the reaction mechanism occurred at the MWCNT/ZLH-LP paste electrode and PCM solution. In a solution, PCM was oxidized electrochemically to produce *N*-acetyl-*p*-quinoneimine (NAPQI) by releasing two electrons and protons, while in an electrode surface, Zn^{2+} from ZLH and anion in an interlayer of ZLH accepting those electrons and protons, respectively, to produce Zn and *L*-phenylalaninediol (LPOH).

Stability and reproducibility

In order to determine the reproducibility of the MWCNT/ZLH-LP paste electrode, the electrochemical responses of 1.0×10^{-4} M PCM were investigated at three modified MWCNT/ZLH-LP paste electrodes freshly fabricated independently. The relative standard deviation (RSD) obtained was 2.83%, suggesting good reproducibility of the proposed paste electrode. Ten replicate measurements of PCM produced RSD of 3.79%. The data showed good consistency of the paste electrode and proved that the proposed paste electrode was not poisoned by PCM oxidation reaction and capable to

Table 2 Detection of PCM in pharmaceutical tablet using the MWCNT/ZLH-LP paste electrode

Sample	Initial (10^{-6} M)	PCM added (10^{-6} M)	PCM detected (10^{-6} M)	Recovery (%)
1.	66.2	0.0	65.4	98.8
2.	66.2	10.0	77.5	101.7
3.	66.2	20.0	88.1	102.2

be used repeatedly. Lastly, the stability of the MWCNT/ZLH-LP paste electrode was investigated by storing in the laboratory at room temperature for 3 weeks. The MWCNT/ZLH-LP paste electrode retained about 96.7% (> 95%) from their initial value indicating the excellent storage stability of the proposed electrode [52].

Interference study

The influences of different potentially interfering compounds on the detection of PCM were evaluated under optimal conditions using 1.0×10^{-4} M PCM. The limit of tolerance was taken as the highest concentration of the interfering species which caused an error of not more than ± 10% from its initial value in the determination of PCM. The data in Fig. 11 shows that the 400-fold concentration of NO_3^-, SO_4^{2-}, Cl^-, and bisphenol A (BPA); the 200-fold of sucrose, fructose, glucose, hydroquinone, and lysine; and the 100-fold of ascorbic acid (AA) and uric acid (UA) did not display interference to the peak currents of PCM.

Real sample analysis

The reliability of the MWCNT/ZLH-LP paste electrode was investigated to determine PCM in pharmaceutical tablets and verify its potential application under optimum conditions. From Table 2, the result shows satisfactory recoveries of PCM with the percentage in the range of 98.8–102.2% which is closed to 100% indicates that the MWCNT/ZLH-LP paste electrode can be applied efficiently for analysis of PCM preparation.

Conclusions

As a conclusion, the MWCNT/ZLH-LP paste electrode was successfully developed by the simple electrochemical approach for PCM determination. The current peaks of the MWCNT/ZLH-LP paste electrode were significantly enhanced compared to the unmodified MWCNT paste electrode due to a higher conductivity and a larger electrochemical active surface area of the proposed paste electrode by adding ZLH-LP modifier. With a wider linear range (7.0×10^{-7} M to 1.0×10^{-4} M), a lower limit of detection (8.3×10^{-8} M), reproducibility, and stability towards PCM determination, the proposed electrode could be used as an alternative method for analysis of PCM in the future.

Funding information The authors would like to thank the Ministry of Higher Education (MOHE), Malaysia, for financial support through a FRGS grant: 2017-0075-101-02 for this work. One of the authors, Mohamad Syahrizal Ahmad is also thankful to Sultan Idris Education University for providing PhD scholarship under SLKKAP scheme.

Compliance with ethical standards

Conflict of interest The authors declare that they have competing interests.

References

1. Bosch ME, Sanchez AJR, Rojas FS, Ojeda CB (2006) Determination of paracetamol: historical evolution. J Pharm Biomed Anal 42(3):291–321
2. Goyal RN, Singh SP (2006) Votammetric determination of paracetamol at C_{60} modified glassy carbon electrode. Electrochim Acta 51(15):3008–3012
3. Prabakar SJR, Narayanan SS (2007) Amperometric determination of paracetomol by a surface modified cobalt hexacyanoferrate graphite wax composite electrode. Talanta 72(5):1818–1827
4. Bessems JGM, Vermeulen NPE (2001) Paracetamol (acetaminophen) induced toxicity: molecular and biochemical mechanisms, analogues and protective approaches. Crit Rev Toxicol 31(1):55–138
5. Olaleye MT, Roch BTJ (2008) Acetaminophen-induced liver damage in mice: effects of some medicinal plants on the oxidative defense system. Exp Toxicol Pathol 59(5):319–327
6. Mazer M, Perrone J (2008) Acetaminophen induced nephrotoxicity: pathophysiology, clinical manifestations, and management. J Med Toxicol 4(1):2–6
7. Lee WM (2013) Drug induced acute liver failure. Clin Liver Dis 17(4):575–586
8. Knochen M, Giglio J, Reis BF (2003) Flow injection spectrophotometric determination of paracetamol in tablets and oral solutions. J Pharm Biomed Anal 33(2):191–197
9. Capella-Petro ME, Bose D, Rubert MF, Esteve Romero J (2006) Optimization of a capillary zone electrophoresis method by using a central composite factorial design for the determination of codeine and paracetamol in pharmaceuticals. J Chromatogr B 839(1-2):95–101
10. Usifoh CO, Adelusi SA, Adebambo RF (2002) Colorimetric determination of paracetamol in raw material and in pharmaceutical dosage forms. Pak J Sci Ind Res 45:7–9
11. Issa YM, Hassoun MEM, Zayed AG (2012) Simultaneous determination of paracetamol, caffeine, domperidone, ergotamine tartrate, propyphenazone and drotaverine HCl by high performance liquid chromatography. J Liq Chromatogr Relat Technol 35:2148–2161
12. Marin A, Barbas C (2004) CE versus HPLC for the dissolution test in a pharmaceutical formulation containing acetaminophen, phenylephrine and chlorpheniramine. J Pharm Biomed Anal 35(4):769–777
13. Wesley CS, Pareira PF, Marra MC (2011) A simple strategy for simultaneous determination of paracetamol and caffeine using flow injection analysis with multiple pulse amperometric detection. Electroanalysis 23:2764–2770
14. Al-Zoubi N, Koundourellis JE, Malamataris S (2002) FTIR and Raman spectroscopic methods for identification and quantitation of orthorhombic and monoclinic paracetamol in powder mixes. J Pharm Biomed Anal 29(3):459–467
15. Rote AR, Kumbhoje PA, Bhambar RS (2012) UV-visible spectrophotometric simultaneous estimation of paracetamol and nabumetone by AUC method in combined tablet dosage form. Pharm Methods 3(1):40–43
16. Sirajuddin AR, Khaskheli A, Shah MI, Bhanger A, Niaz A, Mahesar S (2007) Simpler spectrophotometric assay of paracetamol in tablets and urine samples. Spectrochim Acta A Mol Biomol Spectrosc 68(3):747–751

17. Easwaramoorthy D, Yu YC, Huang HJ (2001) Chemiluminescence detection of paracetamol by a luminal-permanganate based reaction. Anal Chim Acta 439(1):95–100
18. Yang H, Liu B, Ding Y, Li L, Ouyang X (2015) Fabrication of cuprous oxide nanoparticles-graphene nanocomposite for determination of acetaminophen. J Electroanal Chem 757:88–93
19. Chiavazza E, Berto S, Giacomino A, Malandrino M, Barolo C, Prenesti E, Vione D, Abollino O (2016) Electrocatalysis in the oxidation of acetaminophen with an electrochemically activated glassy carbon electrode. Electrochim Acta 192:139–147
20. Vidyadharan AK, Jayan D, Nancy TEM (2014) $Ni_{0.1}Co_{0.9}Fe_2O_4$ based electrochemical sensor for the detection of paracetamol. J Solid State Electrochem 18(9):2513–2519
21. Pournaghi-Azar MH, Kheradmandi S, Saadatirad A (2010) Simultaneous voltammetry of paracetamol, ascorbic acid and codeine on a palladium plated aluminium electrode: oxidation pathway and kinetics. J Solid State Electrochem 14(9):1689–1695
22. Tyszczuk-Rotko K, Beczkowska I, Wojciak-Kosior M, Sowa I (2014) Simultaneous voltammetric determination of paracetamol and ascorbic acid using a boron-doped diamond electrode modified with Nafion and lead films. Talanta 129:384–391
23. Yang G, Wang L, Jia J, Zhou D, Li D (2012) Chemically modified glassy carbon electrode for electrochemical sensing paracetamol in acidic solution. J Solid State Electrochem 16(9):2967–2977
24. Raoof JB, Chekin F, Ojani R, Barari S, Anbia M, Mandegarzad S (2012) Synthesis and characterization of ordered mesoporous carbon as electrocatalyst for simultaneous determination of epinephrine and acetaminophen. J Solid State Electrochem 16(12):3753–3760
25. Iijima S (1991) Helical microtubules of graphitic carbon. Nature 354(6348):56–58
26. Cernat A, Tertis M, Sandulescu R, Bedioui F, Cristea A, Cristea C (2015) Electrochemical sensors based on carbon nanomaterials for acetaminophen detection: a review. Anal Chim Acta 886:16–28
27. Zagal JH, Griveau S, Santander-Nelli M, Granados SG, Bedioui F (2012) Carbon nanotubes and metalloporphyrins and metallophthalocyanines-based materials for electroanalysis. J Porphyrins Phthalocyanines 16(07n08):713–740
28. Wang S, Yang J, Zhou X, Xie J, Ma L, Huang BJ (2014) Electrochemical properties of carbon nanotube/graphene oxide hybrid electrodes fabricated via layer by layer self-assembly. J Electroanal Chem 722:141–147
29. Li H, Pan L, Lu T, Zhan Y, Nie C, Sun ZJ (2011) A comparative study on electrosorptive behavior of carbon nanotubes and graphene for capacitive deionization. J Electroanal Chem 653(1-2):40–44
30. Beitollahi H, Raoof JB, Hosseinzadeh R (2011) Application of a carbon paste electrode modified with 2,7-bis(ferrocenyl ethyl)fluoren-9-one and carbon nanotubes for voltammetric determination of levodopa in the presence of uric acid and folic acid. Electroanalysis 23(8):1934–1940
31. Hashim N, Sharif SNM, Isa IM, Hamid SA, Hussein MZ, Bakar SA, Mamat M (2017) Controlled release formulation of an antidepression drug based on a L-phenylalanate-zinc layered hydroxide intercalation compound. J Phys Chem Solids 105:35–44
32. Yin H, Shang K, Meng X, Ai S (2011) Voltammetric sensing of paracetamol, dopamine and 4-aminophenol at a glassy carbon electrode coated with gold nanoparticles and an organophilic layered double hydroxide. Microchim Acta 175(1–2):39–46
33. Isa IM, Saruddin S, Hashim N, Ahmad M, Ghani SA (2016) Determination of hydrazine in various water samples by square wave voltammetry with zinc-layered hydroxide-3-(4-methoxyphenyl) propionate nanocomposite modified glassy carbon electrode. Int J Electrochem Sci 11:4619–4631
34. Su LH, Zhang XG, Liu Y (2008) Electrochemical performance of Co-Al layered double hydroxide nanosheets mixed with multiwall carbon nanotubes. J Solid State Electrochem 12(9):1129–1134
35. Nicholson RS (1965) Some examples of the numerical solution of nonlinear integral equations. Anal Chem 37(6):667–671
36. Laviron E, Roullier L, Degrand C (1980) A multilayer model for the study of space distributed redox modified electrodes: part II. Theory and application of linear potential sweep voltammetry for a simple reaction. J Electroanal Chem 112(1):11–23
37. Mirceski V, Lovric M (2001) Ohmic drop effects in square-wave voltammetry. J Electroanal Chem 497(1-2):114–124
38. Anson FC (1964) Application of potentiostatic current integration to the study of the adsorption of cobalt (III)-(ethylenedinitrolo(tetraacetate) on mercury electrodes). Anal Chem 36(4):932–934
39. Adams RN (1969) Electrochemistry at solid electrodes. Marcel Dekker, New York
40. Saidin MI, Isa IM, Ahmad M, Hashim N, Kamari A, Ghani SA, Suyanta MS (2016) Square wave anodic stripping voltammetry of copper (II) at a MWCNT paste electrode modified with a tetracarbonylmolybdenum (0) nanocomposite. Microchim Acta 183(4):1441–1448
41. Arvand M, Gholizadeh TM (2013) Simultaneous voltammetric determination of tyrosine and paracetamol using a carbon nanotube-graphene nanosheet nanocomposite modified electrode in human blood serum and pharmaceuticals. Colloids Surf B 103:84–93
42. Holanda LF, Ribeiro FWP, Sousa CP, Casciano PNS, Neto PL, Correia AN (2016) Multi-walled carbon nanotubes-cobalt phthalocyanine modified electrode for electroanalytical determination of acetaminophen. J Electroanal Chem 772:9–16
43. Mao A, Li H, Jin D, Yu L, Hu X (2015) Fabrication of electrochemical sensor for paracetamol based on multi-walled carbon nanotubes and chitosan-copper complex by self-assembly technique. Talanta 144:252–257
44. Li T, Xu J, Zhao L, Shen S, Yuan M, Liu W, Tu Q, Yu R, Wang J (2016) Au nanoparticles/poly(caffeic acid) composite modified glassy carbon electrode for voltammetric determination of acetaminophen. Talanta 159:356–364
45. Liu B, Ouyang X, Ding Y, Luo L, Xu D, Ning Y (2016) Electrochemical preparation of nickel and copper oxides decorated graphene composite for simultaneous determination of dopamine, acetaminophen and tryptophan. Talanta 146:114–121
46. Santos AM, Wong A, Almeida AA, Fatibello-Filho O (2017) Simultaneous determination of paracetamol and ciprofloxacin in biological fluid samples using a glassy carbon electrode modified with graphene oxide and nickel oxide nanoparticles. Talanta 174:610–618
47. Filik H, Avan AA, Aydar S, Cetintas G (2014) Determination of acetaminophen in the presence of ascorbic acid using a glassy carbon electrode modified with poly(caffeic acid). Int J Electrochem Sci 9:148–160
48. Mahmoud BG, Khairy M, Rashwan FA, Banks CE (2017) Simultaneous voltammetric determination of acetaminophen and isoniazid (hepatotoxicity related drugs) utilizing bismuth oxide nanorod modified screen-printed electrochemical sensing platforms. Anal Chem 89(3):2170–2178
49. Tajik S, Taher MA, Baitollahi H (2014) Application of new ferrocene derivative modified graphene paste electrode for simultaneous determination of isoproterenol, acetaminophen and theophylline. Sensors Actuators B Chem 197:228–236
50. Hudari FF, Duarte EH, Pereira AC, Dall'Antonia LH, Kubota LT, Tarley CRT (2013) Voltammetric method optimized by multiresponse assays for the simultaneous measurements of uric acid and acetaminophen in urine in the presence of surfactant using MWCNT paste electrode. J Electroanal Chem 696:52–58

51. Ghica ME, Ferreira GM, Brett CMA (2015) Poly(thionine) carbon nanotube modified carbon film electrodes and application to the simultaneous determination of acetaminophen and dipyrone. J Solid State Electrochem 19(9):2869–2881

52. Ensafi AA, Ahmadi N, Rezaei B, Abarghoui MM (2015) A new electrochemical sensor for the simultaneous determination of acetaminophen and codeine based on porous silicon/palladium nanostructure. Talanta 134:745–753